

Accelerated recombination due to resonant deexcitation of metastable states

Yuri V. Ralchenko and Yitzhak Maron

Faculty of Physics, Weizmann Institute of Science, Rehovot 76100, Israel

Abstract

In a recombining plasma the metastable states are known to accumulate population thereby slowing down the recombination process. We show that an account of the doubly-excited autoionizing states, formed due to collisional recombination of metastable ions, results in a significant acceleration of recombination. A fully time-dependent collisional-radiative (CR) modeling for stripped ions of carbon recombining in a cold dense plasma demonstrates an order of magnitude faster recombination of He-like ions. The CR model used in calculations is discussed in detail.

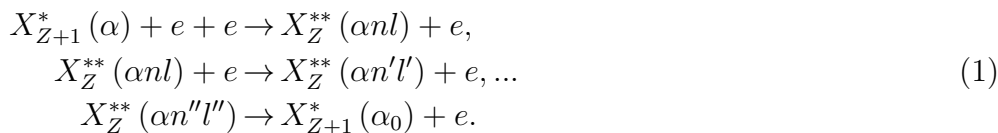
1 Introduction

Recombination of atomic ions in plasmas [1] continues to be a subject of a permanent interest. Recent measurements of radiative recombination cross sections for various ions, including the simplest bare ions (see, e.g., Ref. [2] and references therein), have shown a noticeable and surprising disagreement between theory and experiment. In addition to such fundamental issues, various phenomena related to recombination play important roles in plasma kinetics [3]. A well-known example is provided by a recombination-based formation of population inversion used for practical lasing in the soft X-ray region [4].

In spite of a widely recognized importance of ion recombination for plasma evolution, the theoretical efforts were hitherto directed practically only to the recombinational kinetics of (quasi-)hydrogenic ions while non-hydrogenic recombination was only scarcely studied [5,6]. As far as recombination is concerned, the major difference between hydrogenic and non-hydrogenic ions is the possible presence of long-lived metastable states in the energy spectrum of the latter. The metastable states accumulate the downward flowing population for times of the order of the inverse depopulation rates. Since this rate could be rather small, the population accumulation would therefore exist for

relatively long times. The purpose of this paper is to demonstrate that the process of the so-called "resonant deexcitation" (RD) can significantly alter this picture and, in fact, accelerate the overall recombination process by as much as an order of magnitude.

The resonant deexcitation, as it is defined here, proceeds in three steps. First, a free electron is collisionally captured by an *excited* ion with the spectroscopic charge $Z+1$ to form a doubly-excited state of the ion Z . This step is a familiar collisional 3-body recombination which though originates from excited rather than ground state of an ion. In the second step, the captured electron may move upward or downward between high- n states due to collisional excitation or deexcitation. Finally, the doubly-excited state decays via autoionization thereby producing an ion with the charge $Z+1$, so that the initial and final states of RD belong to the same ion stage. The total chain of elementary events, i.e., recombination, (de)excitation and autoionization, looks as follows:



Here α denotes the quantum state of the initial excited ion, nl are the principal and orbital quantum numbers of the captured electron, and α_0 is the set of the final quantum numbers. The final state $X_{Z+1}^*(\alpha_0)$ may obviously be also an excited one (rather than only the ground state) provided the energy difference between initial and final states of the $Z+1$ ion is larger than the ionization energy of the $n''l''$ electron. The doubly-excited quantum states $X_Z^{**}(\alpha nl)$ with different nl form a shifted Rydberg series with the ionization limit $X_{Z+1}^*(\alpha)$.

The effect of RD on level populations was independently recognized by Fujimoto and Kato [7] and by Jacoby *et al.* [8] (with respect to the X-ray laser problem). Later and independently, Koshelev with colleagues [9,10] discussed the population of doubly-excited levels via 3-body recombination from excited states. The primary interest in these papers was directed towards either hydrogen-like ions [7,8] or production of dielectronic satellites [9,10], and therefore the importance of RD for recombination of non-hydrogenic ions was not investigated. Moreover, it was found [8] that the RD channel

$$n = 3 \rightarrow 3lnl' \rightarrow 1s + e \tag{2}$$

in the recombining H-like C VI plasma is negligibly small comparing to the direct radiative decay $n = 3 \rightarrow n = 1$. Then, in a recent series of papers Kawachi *et al.* [11] investigated a quasi-steady-state recombination of Li-like Al and showed that accounting for RD results in a better agreement with experimental data. It should be noted that some groups [7,11] refer to the

described above process of Eq. (1) as the "DL-deexcitation" which originates from the inverse process of dielectronic capture and ladder-like excitation. Here the term "resonant deexcitation" is preferred since no dielectronic capture is involved in the process considered.

The paper is organized as follows. Section II contains a detailed description of the collisional-radiative model used in the simulations. We describe the major kinetic processes taken into account and indicate the sources of atomic data. The calculational results for time-dependent recombination of carbon nuclei and discussion are presented in Section III. Finally, Section IV contains conclusions.

2 Collisional-Radiative Model

The experimental installations at the Plasma Laboratory of the Weizmann Institute of Science (coaxial and planar plasma opening switches and Z-pinch) produce plasmas with diverse and fast-changing properties. The computational tools required for reliable diagnostics of such systems should therefore both reflect a variety of physical processes happening in plasmas and consistently describe the temporal behavior of plasma characteristics under very different conditions. The collisional-radiative (CR) package NOMAD was developed to provide reliable spectroscopic diagnostics of transient plasmas with an arbitrary electron energy distribution function. It includes an executable code and a number of atomic databases containing various related data for many elements and their ions. A convenient user-friendly interface relies upon the usage of common Web browsers and provides both textual and graphical options for the processing of calculated results. The program was written in Fortran 77 with minor extensions from Fortran 90. Presently, the code is running on a 450 MHz Pentium III personal computer with typical run times of the order of several minutes.

Generally, the CR code solves the following first-order system of inhomogeneous differential equations:

$$\begin{aligned} \frac{d\hat{N}(t)}{dt} &= \hat{A}(N_i, N_e, f_e, t) \hat{N}(t) + \hat{S}(t), \\ \hat{N}(t=0) &= \hat{N}_0, \end{aligned} \tag{3}$$

where $\hat{N}(t)$ is the vector of atomic state populations, $\hat{A}(N_i, N_e, f_e, t)$ is the rate matrix depending on ion density $N_i(t)$, electron density $N_e(t)$ and electron-energy distribution function $f_e(E, t)$, and $\hat{S}(t)$ is the source function. The

electron density can be presented as a sum of two components:

$$N_e(t) = N_e^0(t) + N_i(t) \sum_{Z=Z_{min}}^{Z_{max}} (Z-1) \sum_{k=1}^{k_{max}} N_{Z,k}(t), \quad (4)$$

where $N_e^0(t)$ is the background electron density and the second term represents the density of continuum electrons originating from ionization of atoms. In Eq. (4) Z_{min} and Z_{max} are the minimal and maximal spectroscopic charges, index k enumerates the levels within a specific ion with charge Z ($k = 1$ is the ground state etc.), and $N_{Z,k}(t)$ is the population of the corresponding atomic level. The level populations are usually normalized:

$$\sum_{Z=Z_{min}}^{Z_{max}} \sum_{k=1}^{k_{max}} N_{Z,k}(t) = 1, \quad (5)$$

although for calculations with the source function $\hat{S}(t)$ this condition should be discarded. The number of atomic states used in specific calculations can be chosen depending upon the complexity of a task. There are no fundamental limitations on the nature of the states involved, and therefore atomic terms, levels (fine structure components) or configurations can be equally used in the CR calculations if necessary¹. In addition, an arbitrary number of high- n Rydberg states can be added to each of the ion charge states. The highest in energy bound state is determined by the ionization potential lowering. This effect may be accounted for in different approximations using Debye-Huckel, hybrid (Stewart-Pyatt) or ion-sphere formulas [12]. However, an explicit account of numerous Rydberg states essentially increases the calculation time and thus is not always practical. In this case, an effective aggregate state, which is composed of Rydberg states up to the highest bound state, may be used in calculations.

As was already mentioned above, the model allows for use of an arbitrary electron-energy distribution function (EEDF). Usually, the EEDF is first to have been calculated with a coupled hydrodynamic plasma code and then utilized for a detailed CR modeling. It is possible, nevertheless, to approximate this very complicated problem by using simplified EEDFs, for example, Maxwellian+beam or a two-Maxwellian distribution. To this end, the EEDF $f(E)$ is presented as:

$$f(E) = (1 - \alpha) f_M(T_e, E) + \alpha f'(E), \quad (6)$$

where $f_M(T_e, E)$ is the Maxwellian EEDF with an electron temperature T_e , $f'(E)$ is either the beam or the second Maxwellian EEDF, and $0 \leq \alpha \leq 1$ is

¹ Below we use the terms "state" and "level" interchangeably.

the weight of $f'(E)$ in the total EEDF. A modeling with an arbitrary EEDF poses a serious restriction on the data used for the calculation of rates of atomic processes, namely, cross sections rather than Maxwellian-averaged rate coefficients have to be used in calculations.

The atomic processes which affect the level populations and are considered in our model include spontaneous radiative decays, electron-impact collisional processes (excitation, deexcitation and ionization), various types of ion recombination (3-body, radiative and dielectronic recombination), autoionization and dielectronic capture, atom-ion or ion-ion charge exchange, and laser photopumping. The plasma opacity effects are taken into account as well. The atomic data (either raw or fitted with physically justified formulas) are stored in databases, one per element, and the data accuracy is carefully evaluated.

The energy levels and radiative oscillator strengths are mainly collected from available publications and online databases². Whenever these sources cannot provide a necessary level of accuracy and/or completeness, the missing energies and oscillator strengths are calculated with various atomic software, e.g., RCN/RCN2/RCG Hartree-Fock package [14], MZ 1/Z-expansion code [15], or GRASP92 multiconfiguration Dirac-Fock code [16].

The electron-impact collisional data comprise a majority of atomic data utilized in CR calculations. The existing data on cross sections are rather incomplete and mostly cover excitations and ionizations from ground states. Hence, production of new cross sections becomes a necessity if a detailed diagnostics is required. Our main source of excitation data is the Coulomb-Born-exchange unitarized code ATOM [15] which combines a high calculational speed with a good accuracy, especially for moderately- and highly-ionized atoms. Previously we have shown that ATOM excitation data for H- and Li-like ions very well agree with the cross sections calculated by the more sophisticated convergent close-coupling (CCC) method [17,18]. Nevertheless, a use of more precise data is made whenever possible; for example, our database of collisional cross sections for neutral Helium was developed using the latest recommended CCC fits [19]. For comparison purposes or when no other data are available, a simple van Regemorter formula for excitation cross sections may be utilized as well. The inverse, deexcitation cross sections are obtained using the detailed balance principle, the former being implemented also for calculation of other inverse cross sections from the direct ones (e.g., 3-body recombination from ionization etc.).

The fits for the electron-impact ionization cross sections from ground states were obtained using the recommended data compiled by the Belfast group [20,21] with account of corrections discussed in Ref. [22]. Presently, four op-

² A list of Internet atomic databases can be found in [13].

tions for calculation of the ionization cross sections from excited states are available, namely: (i) ATOM data, (ii) Lotz formula [23], (iii) l -dependent semiempirical formula [24], and (iv) simple classical scaling

$$\sigma(E/I) = \frac{I_0^2}{I^2} \sigma_0(E/I_0) \quad (7)$$

with I and I_0 being the corresponding ionization energies from excited and ground states, respectively. The single ionization is allowed to proceed into both ground and excited states of the next ion. The multiple ionization which may be very important for non-equilibrium plasmas, especially in the presence of high-energy electrons, is also taken into account. The corresponding cross section connecting ground states of respective ions is calculated with recommended formulas from Ref. [25].

The photoionization cross sections, which are also used for calculation of radiative recombination data with the Milne formula, are compiled from a few sources, such as Opacity Project [26], ATOM calculations or other published compilations and evaluations [27,28]. The less accurate hydrogenic Kramers formulas are used to calculate the photorecombination into the high- n Rydberg states and/or the aggregate state.

The dielectronic recombination can be taken into account in two ways. One method consists in an explicit treatment of autoionizing states with a use of dielectronic capture cross sections and autoionization transition probabilities. The latter are usually calculated with the MZ or Cowan's [14] codes and the former are obtained using the principle of detailed balance. Furthermore, the collisional and radiative transitions to, from, and between all doubly-excited autoionizing states are fully accounted for. In the second, less detailed approach, no autoionizing states are presented in the CR calculations, and the dielectronic recombination rates are calculated using one of the existing methods, namely, the modified Burgess formula [14], fitting formulas of Hahn [29], or recent recommended fits from Ref. [30].

A two-step procedure is implemented in treatment of the plasma opacity effects. First, when calculating the level populations, a simple escape factor method is applied. The dependence of the escape factor on optical depth is calculated using (i) the fitting formulas produced for a general Voigt line profile with the Monte-Carlo code TRACE [31] or (ii) Apruzese's formulas for the Voigt escape factor [32]. Then, on the second step, when an actual spectrum is synthesized, the radiation transfer equation for a Voigt profile is solved for each of the selected spectral lines using the level populations obtained from the rate equations. The Voigt line profile is constructed from Doppler (Gaussian) and natural+Stark (Lorentz) broadening parts. The Doppler width is determined by the ion temperature T_i which may be another independent in-

put parameter. The depopulating rates from both lower and upper levels of specific radiative transitions are used to calculate the inelastic Stark width, and the elastic Stark linewidth is ignored because of its steep decrease with electron temperature and small contribution for moderate to high temperatures (see Refs. [33,34] for discussion on elastic contribution). Finally, it is worth noting that Drayson's routine [35] is used in the generation of Voigt profile.

3 Results and discussion

To study the effect of resonant deexcitation on kinetics of recombination, we consider here the time-dependent recombination of fully stripped ions of carbon in an optically thin cold dense plasma. This situation may be experimentally implemented, for instance, when a beam of bare ions is injected into a pre-formed plasma. The recombination of carbon nuclei has already been a subject of discussion at the NLTE kinetics workshop [36]; however, emphasis was given to the most general plasma characteristics such as mean ion charge and therefore no detailed examination of the evolution of level populations was carried out.

In the present calculation all charge states of carbon from neutral atom up to the fully stripped ion were retained. The basic atomic states were mainly the atomic terms characterized by the total angular momentum and spin. The exceptions are the following: (i) the $1s2l\ ^3P$ term in C V is split into the fine structure components, (ii) the doubly-excited autoionizing states in Li-like C IV and He-like C V are represented by the configurations $1s2lnl'$ (total of 15 states up to $1s2s8l$ and $1s2p8l$) and $2lnl'$ (7 states up to $n = 8$), and (iii) l -summed states characterized only by the principal quantum number are used in H-like C VI. Besides, 20 high- n Rydberg states were added to each of the ion charge states. However, the actual number of Rydberg states becomes smaller since the ionization potential lowering effectively cuts off the bound spectrum. The total number of atomic states was about 180.

The CR calculations were performed for two cases differing in the number (and nature) of included states. In the first case (A), the doubly-excited autoionizing states for C IV and C V are excluded from consideration, and thus the resonant deexcitation channel is closed. Nevertheless, we do account for the process of dielectronic recombination using the rates recommended by Hahn [29]. It is worth mentioning that this type of ion recombination is essentially unimportant for the low temperatures and high densities specific for the problem in question. In the second case (B), 22 doubly-excited states in C IV and C V listed above were added with a detailed account of all relevant atomic processes (autoionization, dielectronic capture, ionization, 3-body recomb-

nation, radiative decays, and excitation/deexcitation). The electron impact excitation and deexcitation cross sections between these levels were calculated in the van Regemorter approximation, while the relevant radiative and autoionization probabilities were determined with the MZ code. In addition, the collisional and radiative (satellite) transitions of the core electron, e.g., $1s2pnl \rightarrow 1s^2nl + h\nu$, were also taken into account.

For each of the cases A and B, the CR simulations were carried out for several sets of electron density N_e and temperature T_e . Below we mainly discuss the plasma evolution for $N_e = 3 \times 10^{19} \text{ cm}^{-3}$ and $T_e = 3 \text{ eV}$, and comparison with other sets is given when necessary³. Both electron density and temperature were kept constant during the run. The initial population distribution and temporal history were set as following. At time $t = 0$ all population is in the bare nucleus of carbon, and the logarithmic time mesh for basic conditions is chosen according to:

$$\begin{aligned} t_0 &= 0; t_1 = 10^{-16} \text{ s}, \\ i > 1 : t_i &= t_{i-1} * 1.11344, \end{aligned} \quad (8)$$

so that $t_{150} = 10^{-9} \text{ s}$. This final time was found to be sufficient to reach the CR equilibrium (CRE) state for both sets of calculations (A and B). For other than basic conditions, the logarithmic time mesh was properly adjusted in order to achieve CRE within 150 steps.

Consider first the calculated evolution of level populations for case A (no doubly-excited autoionizing states). The total populations of all charge states of carbon as a function of time are shown by the solid lines in Fig. 1. The mostly noticeable feature in this plot is a very long lifetime of the He-like C V ion, $t \simeq 10^{-10} \text{ s}$, which exceeds the lifetime of C IV. To examine how the metastable states 2^3S and $2^3P_{0,2}$ affect the C V lifetime, let us compare the populations of all $n = 1$ and $n = 2$ states of C V and the total C V population (Fig. 2(a)). Note that the components of the 2^3P term are in local thermodynamic equilibrium (LTE) due to high collisional rates. The sum of populations of the triplet states $N(2^3S) + \sum_{j=0..2} N(2^3P_j)$ shown by the solid line with squares nearly coincides with the total C V population after $t \simeq 1.5 \times 10^{-11} \text{ s}$ which indicates that the lifetime of C V is indeed governed by the $n = 2$ triplet levels. The radiative decay of the triplet levels to the ground state is negligibly small comparing to the collisional deexcitation rates which for basic conditions are $2.3 \times 10^9 \text{ s}^{-1}$ for 2^3S and $1.9 \times 10^{10} \text{ s}^{-1}$ for the 2^3P term. These values are by factor 3.3 and 2.5, respectively, smaller than the highest collisional rates between the $n = 2$ triplet and singlet levels: $7.8 \times 10^9 \text{ s}^{-1}$ for $2^3S \rightarrow 2^1S$ and $4.9 \times 10^{10} \text{ s}^{-1}$ for $2^3P \rightarrow 2^1P$. This, together with

³ This particular set of plasma parameters will be referred to as the "basic conditions".

the high collisional rates within the triplet and singlet subsystems and strong radiative decay $2^1P \rightarrow 1^1S$ with the probability $A \approx 8.9 \times 10^{11} \text{ s}^{-1}$, shows that the characteristic depopulation time of the triplet levels is mainly determined by the triplet-singlet collisional transitions followed by a fast radiative decay of the 2^1P state.

The long lifetime of C V results in a relatively low peak populations of the C IV and C III ions (see Fig. 1). As a result, both C V and C II simultaneously have high populations during a long time of the order of 10^{-10} s. Had such a picture of coexisting ion states with very different charges be true, it would allow for a new scheme of laser photopumping when, e.g., the photons from the $2^3S - 2^3P$ transition in a long-living He-like ion would pump a transition with the same wavelength in another low-charge ion, thereby giving rise to a possible population inversion. However, the detailed calculations for the case B disallow such a possibility.

The case B calculations which were performed with an explicit account of autoionizing states show a remarkably different temporal behavior of the total ion populations (dashed lines in Fig. 1). Recalling that the doubly-excited autoionizing states were added to both He- and Li-like ions, one may notice the earlier appearance of the He-like ion comparing to case A. However, the lifetime of the H-like ion decreases only by less than 30% due to the RD channel $n = 2 \rightarrow n = 1$. This indicates that for the basic conditions the resonant deexcitation of the $n = 2$ state of C VI can hardly compete with its strong radiative decay to the ground $n = 1$ state. The temporal history of the He-like and other ion stages is, on the other hand, drastically different from the case A calculations. As is seen from Fig. 1, the lifetime of C V in case B is an order of magnitude smaller due to a much faster decay of the metastable states resulting from the resonant deexcitation. The effect of a strong depopulating RD channel can be clearly seen in Fig. 2(b), where the populations of $n = 1$ and all $n = 2$ states for case B are presented. One can notice that both 2^3S and 2^3P_j states have now populations smaller than that of the ground state while in case A their populations exceed that of the ground state by about two orders of magnitude. Furthermore, due to a much larger population flux from C V, the peak populations of C IV and C III are now significantly larger (Fig. 1). Thus, one can see that account of resonant deexcitation of the metastable levels in C V leads to drastic changes in evolution of different ions.

The physical picture of resonant deexcitation is quite straightforward. The highest- n states are quickly populated from the metastable states due to high 3-body recombination rates. The radiative decay of the core electron $2p \rightarrow 1s$ does not depend significantly on n as long as n is sufficiently high. The rates of autoionization $1s2lnl' \rightarrow 1s^2 + \epsilon l''$ are lower for higher principal quantum numbers ($A_a(n) \sim n^{-3}$), and so are the radiative transition probabilities of the outer electron. For dense low-temperature plasmas the main channel of

depopulation for the highest- n states is a ladder-like collisional deexcitation to lower doubly-excited states. When the population flow reaches those states for which the autoionization probability is comparable or larger than the deexcitation rate, the downward flow is redirected into the C V ground state, so that the lowest doubly-excited states have small populations.

An approximate formula for the RD rate can be found assuming that the populations for the doubly-excited autoionizing states above the so-called "thermal limit" [9] are in the Saha-Boltzmann equilibrium with their "parent" excited state of the next ion [8]. The thermal limit is defined as the state for which the rate of collisional processes is of the order of autoionization probability, and the corresponding principal quantum number n_{th} for the thermal limit may be estimated from the expression [9]:

$$n_{th} \simeq 300 \times \frac{Z^{2/9} T^{1/9}}{N_e^{1/9}} p^{4/9}, \quad (9)$$

where p is the principal quantum number of the excited state of the recombining ion. The value of n_{th} is obviously a very weak function of plasma parameters, and for the basic conditions and $p = 2$ one has $n_{th} \simeq 4$. Thus, the RD rate can be determined from the following equation:

$$\begin{aligned} N_{Z+1}(\alpha) R_{RD}(\alpha - \alpha_0) &= \sum_{n \geq n_{th}}^{n_{max}} N_Z(\alpha n l) A(\alpha n l - \alpha_0) \\ &= N_{Z+1}(\alpha) N_e \left(\frac{2\pi \hbar^2}{m T_e} \right)^{3/2} \frac{1}{2g(\alpha)} \\ &\quad \times \sum_{n \geq n_{th}}^{n_{max}} e^{Z^2 Ry/n^2 T_e} g(\alpha n l) A(\alpha n l - \alpha_0) \end{aligned} \quad (10)$$

where $N_{Z+1}(\alpha)$ is the population of the initial (excited) state α with the statistical weight $g(\alpha)$, $N_Z(\alpha n l)$ is the population of the doubly-excited state formed by a capture of the continuum electron into atomic level with quantum numbers n and l and $g(\alpha n l)$ is its statistical weight, and $A(\alpha n l - \alpha_0)$ is the probability of the autoionization process $(Z, \alpha n l) \rightarrow (Z + 1, \alpha_0) + e$. The summation is extended above the thermal limit up to the highest bound doubly-excited state with the principal quantum number n_{max} which is determined by the ionization potential lowering. Here we assume that the ionization energies of the autoionizing states are given by the hydrogen-like formula $I_n = Z^2 Ry/n^2$ with $Ry = 13.61$ eV being the Rydberg energy. For low temperatures, which are the subject of the present work, the first term in this sum with $n = n_{th}$ gives an overwhelming contribution due to a strong exponential dependence on n . In agreement with this conclusion our modeling shows that the doubly-excited states $1s2l3l'$ and $1s2l4l'$ indeed provide the largest

contribution to resonant deexcitation.

Retaining only the first term in Eq. (10) and using a well-known expression for autoionization probability in terms of the excitation cross section at threshold (see, e.g., [15]), we obtain the following formula for the RD rate :

$$R_{RD}(\alpha - \alpha_0) = N_e \frac{g(\alpha_0)}{g(\alpha)} \frac{4\bar{g}f_{\alpha_0\alpha}}{\sqrt{3}\Delta E_{\alpha_0\alpha}} \frac{Z^2 Ry^2}{\hbar n_{th}^3} \left(\frac{2\pi\hbar^2}{mT_e}\right)^{3/2} \exp\left(\frac{Z^2 Ry}{n_{th}^2 T_e}\right) \\ \approx 2 \times 10^{-6} \frac{g(\alpha_0)}{g(\alpha)} \frac{N_e (cm^{-3})}{n_{th}^3 T_e^{3/2} (eV)} \exp\left(\frac{13.6 \cdot Z^2}{n_{th}^2 T_e (eV)}\right). \quad (11)$$

To derive the second equation, we use the values of $\Delta E_{\alpha_0\alpha} = 3/4 \cdot Z^2 Ry$ for the transition energy (for He- and H-like ions), $f_{\alpha_0\alpha} = 0.5$ for the corresponding oscillator strength for the transition $(Z, \alpha_0) - (Z, \alpha)$, and $\bar{g} = 0.2$ for the threshold value of the Gaunt factor. Using Eq. (9) for n_{th} , one has:

$$R_{RD}(\alpha - \alpha_0) \approx 2.9 \times 10^{-14} \frac{g(\alpha_0)}{g(\alpha)} \frac{N_e^{4/3}}{Z^{2/3} T_e^{11/6}} \exp\left(8 \times 10^{-5} \frac{Z^{16/9} N_e^{2/9}}{T_e^{10/9}}\right). \quad (12)$$

Thus, the RD rate for low-temperature plasmas shows a strong dependence on electron temperature (cf. $T_e^{-4.5}$ behavior of the 3-body recombination rate) and a moderate, slightly stronger than linear, dependence on electron density. The T_e -dependence is illustrated in Fig. 3 where we present the time evolution of carbon charge states for $T_e = 2, 5$ and 10 eV and a constant density of $N_e = 3 \times 10^{19} \text{ cm}^{-3}$. It is clearly seen that the difference between the simulations with (solid lines) and without (dashed lines) RD is mostly noticeable for the lowest of temperatures while for $T_e = 10$ eV both sets of calculations produce almost identical evolution of charge states.

The effective RD rate calculated from Eq. (12) is about $6 \times 10^{12} \text{ s}^{-1}$ for the basic conditions. This value seems to disagree with the results of the detailed modeling (Fig. 1) for C V where the characteristic decay time is of the order of 10^{-11} s . Such a discrepancy may be in part due to strong deviations from the Saha-LTE regime for the doubly-excited states during the fast recombination which is considered here. Our calculations show that during the time when C V is mostly abundant, only the highest autoionizing states $1s2l8l'$ (and $1s2l7l'$ to a lesser extent) have Saha populations while the others deviate strongly from the respective Saha limits. As for the $1s2l3l'$ and $1s2l4l'$ states which mostly contribute to resonant deexcitation, their populations differ by as much as a factor of 5. Nevertheless, a use of the effective RD rate from Eq. (12) in CR calculations *without* doubly-excited states results in charge state evolution which is rather close to that obtained from the detailed simulations with autoionizing states and RD included (case B). The charge state

populations shown in Fig. 4 were calculated for these two cases for $N_e = 10^{20}$ cm^{-3} and $T_e = 5$ eV. (Similar results are obtained for other sets of plasma parameters.) One can see that both characteristic decay times and peak ion populations are reproduced within a few tens of percent. It is interesting to note that this situation is similar to the coronal approximation where line intensities do not depend on the radiative decay probability and are determined only by the collisional excitation rates. In the present case, the RD rate is equivalent to the radiative rate while the flux of population coming from the upper states due to cascades is analogous to excitation in corona. Thus, as long as the rate of resonant deexcitation from metastable states exceeds other depopulation rates, the population flux downward is determined only by the cascade contribution and thus is not too sensitive to the actual value of the RD rate.

4 Conclusions

Although resonant deexcitation is already known for a long time, its significance for plasma kinetics does not seem to have been fully appreciated so far. A particular problem of recombination of ions with metastable states shows that a consistent account of resonant deexcitation via the doubly-excited autoionizing states, which are collisionally populated from the excited states of the next ion, can considerably alter the entire picture of recombination. This process may be important, for instance, in kinetics of recombination lasers or for beam-stopping problems. It would certainly be interesting to conduct experiments that could test the conclusions made in the present paper.

5 Acknowledgments

The collaboration with V. Tsitrin on the early stages of this work is highly appreciated. We are grateful to K. N. Koshelev for interesting discussions and to H. R. Griem for valuable comments and reading of the manuscript. Special thanks are due to V. I. Fisher for his help in development of the CR model. The assistance of V. A. Bernshtam, A. Goldgirsh and A. Starobinets in development of atomic databases is highly appreciated. This work is supported part by the Minerva foundation (Munich, Germany) and Israeli Ministry of Absorption.

References

- [1] Recombination of Atomic Ions, ed. by W. G. Graham et al, NATO ASI Series B: Physics Vol. 296 (Plenum Press, New York and London, 1992).
- [2] Müller A. Phil Trans Royal Soc London 1999; A357:1279-96.
- [3] Griem HR. Principles of Plasma Spectroscopy. Cambridge: Cambridge Univ. Press, 1997.
- [4] Elton RC. X-Ray Lasers. New York: Academic Press, 1990.
- [5] Cacciatore M, Capitelli M. Z Naturforsch 1976; 31a:362-8.
- [6] Gorse C, Cacciatore MA, Capitelli M. Z Naturforsch 1978; 33a:895-902.
- [7] Fujimoto T, Kato T. Phys Rev Lett, 1982; 48:1022-25; Phys Rev 1985; A32:1663-8.
- [8] Jacoby D, Pert GJ, Shorrock LD, Tallents GJ. J Phys 1982; B15:3557-80.
- [9] Koshelev KN. J Phys 1989; B21:L593-6.
- [10] Koshelev KN, Rosmej (Yartseva) ON, Rosmej FB, Hebach M, Schulz A, Kunze H-J. J Phys 1992; B25:L243-7.
- [11] Kawachi T, Fujimoto T. Phys Rev, 1997; E55:1836-42; Kawachi T, Ando K, Fujikawa C, Oyama H, Yamaguchi N, Hara T, Aoyagi Y. J Phys 1999; B32:553-62.
- [12] Murillo MS, Weisheit JC. Phys Rep 1998; 302:2-65.
- [13] URL <http://plasma-gate.weizmann.ac.il/DBfAPP.html>.
- [14] Cowan RD. The Theory of Atomic Structure and Spectra. Berkeley: University of California Press, 1981.
- [15] Shevelko VP, Vainshtein LA. Atomic Physics for Hot Plasmas. Bristol: IOP Publishing, 1993.
- [16] Parpia FA, Fischer CF, Grant IP. Comp Phys Comm 1996; 94:249-271.
- [17] Fisher VI, Ralchenko YuV, Bernshtam VA, Goldgirsh A, Maron Y, Golten H, Vainshtein LA, Bray I. Phys Rev 1997; A55:329-34;
- [18] Fisher VI, Ralchenko YuV, Bernshtam VA, Goldgirsh A, Maron Y, Vainshtein LA, Bray I. Phys Rev 1997; A56:3726-33.
- [19] Ralchenko YuV, Janev RK, Kato T, Fursa DV, Bray I, de Heer FJ. Report NIFS-DATA-59, 2000.
- [20] Bell KL, Gilbody HB, Hughes JG, Kingston AE, Smith FJ. J Phys Chem Ref Data 1983; 12:891-916.
- [21] Lennon MA, Bell KL, Gilbody HB, Hughes JG, Kingston AE, Murray MJ, Smith FJ. J Phys Chem Ref Data 1988; 17:1285-1363.
- [22] Kato T, Masai K, Arnaud M. Report NIFS-DATA-14, 1991.

- [23] Lotz W. Z Phys 1967; 206:205-211.
- [24] Bernshtam VA, Ralchenko YuV, Maron Y. J Phys 2000; B33:5025-32.
- [25] Fisher V, Ralchenko YuV, Goldgirsh A, Fisher D, Maron Y. J Phys 1995; B28:3027-46.
- [26] URL <http://vizier.u-strasbg.fr/OP.html>.
- [27] Verner DA, Ferland GJ, Korista KT, Yakovlev DG. Astrophys J 1996; 465:487-98.
- [28] Clark REH, Cowan RD, Bobrowicz FW. At Data Nucl Data Tables 1986; 34:415-22.
- [29] Hahn Y. JQSRT, 1993; 49:81-94.
- [30] Mazzotta P, Mazzitelli G, Colafrancesco S, Vittorio N. Astr Astroph Suppl Ser 1998; 133:403-9.
- [31] Schulz A. PhD thesis, Ruhr-Universitat Bochum, 1990.
- [32] Apruzese JP. JQSRT 1985; 34:447-452.
- [33] Griem HR, Ralchenko YuV, Bray I. Phys Rev 1999; E60:6241.
- [34] Ralchenko YuV, Griem HR, Bray I, Fursa DV. Phys Rev 1999; A59:1890-5.
- [35] Drayson SR. JQSRT 1976; 16:611-7.
- [36] Lee RW, Nash JK, Ralchenko Y. JQSRT 1997; 58:737-42.

Figure Captions

Figure 1. Temporal history of carbon charge states for $N_e = 3 \times 10^{19} \text{ cm}^{-3}$ and $T_e = 3 \text{ eV}$. Solid lines – case A, dashed lines – case B.

Figure 2. Time-dependent populations of the $1s^2$ and $1s2l$ states and C V ion for $N_e = 3 \times 10^{19} \text{ cm}^{-3}$ and $T_e = 3 \text{ eV}$. (a) - case A, (b) - case B. The total population of $n = 2$ triplet states is shown by a solid line with squares.

Figure 3. Temporal history of carbon charge states for $N_e = 3 \times 10^{19} \text{ cm}^{-3}$ and $T_e = 2, 5, \text{ and } 10 \text{ eV}$. Solid lines – case A, dashed lines – case B.

Figure 4. Temporal history of carbon charge states for $N_e = 1 \times 10^{20} \text{ cm}^{-3}$ and $T_e = 5 \text{ eV}$. Solid lines – calculations with effective resonant deexcitation rates, dashed lines – full calculations with autoionizing states included (case B).

